

## Microstructure Evolution and Model Analysis of Al<sub>2</sub>O<sub>3</sub>/ZrO<sub>2</sub> Hypoeutectic Ceramic During Rapid Solidification

Zhonghai Xu<sup>a</sup>, Yongting Zheng<sup>a\*</sup>, Yangyang Guo<sup>a</sup>, Wei Ye<sup>a</sup>, Pan Yang<sup>a</sup>

<sup>a</sup>Center for Composite Materials and Structures, Harbin Institute of Technology, Harbin, PR China

Received: November 24, 2014; Revised: October 12, 2015

Rapid solidification of the super high-temperature Al<sub>2</sub>O<sub>3</sub>/ZrO<sub>2</sub> melt was studied by a novel method. The melt was prepared by explosion reaction using Al and Zr(NO<sub>3</sub>)<sub>4</sub> as raw materials and then sprayed to Cu-plate. The heat transfer during the solidification process was analyzed by one-dimensional Finite Element Analysis. The cooling rate of the melt decreased with the increasing distance from the Cu-plate. According to the microstructure evolution, the coating can be divided into four areas: amorphous, nano-crystalline, cellular and dendrite crystal layer. The amorphous and nano-crystalline (50~100 nm) layers can be obtained at the cooling rate of about 1.68~7.76 × 10<sup>5</sup>K/s and 0.48~1.68 × 10<sup>5</sup>K/s, respectively, while the cooling rate of the cellular and dendrite crystal layers were about 0.26~0.48 × 10<sup>5</sup>K/s and 0.14~0.26 × 10<sup>5</sup>K/s, respectively. The microstructure of the hypoeutectic ceramics shows that the nano-crystalline, cellular and dendritic crystals of the Al<sub>2</sub>O<sub>3</sub> phases were embedded in the Al<sub>2</sub>O<sub>3</sub>/ZrO<sub>2</sub> eutectic matrix.

**Keywords:** combustion synthesis, microstructure evolution, model analysis, Al<sub>2</sub>O<sub>3</sub>/ZrO<sub>2</sub>, thermal explosion spraying, rapid solidification

### 1. Introduction

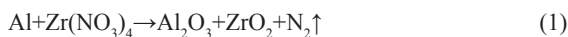
Al<sub>2</sub>O<sub>3</sub>-ZrO<sub>2</sub> eutectic ceramics have a good combination of physical, thermal and mechanical properties, such as ultra-high hardness, excellent oxidation resistance and strength retention at elevated temperatures<sup>1-3</sup>. These excellent properties make Al<sub>2</sub>O<sub>3</sub>-ZrO<sub>2</sub> eutectic ceramics potential for a wide range of applications. Generally, eutectic ceramics were mostly prepared by Bridgman method<sup>3</sup>, laser heated floating zone method<sup>4,5</sup>, micro pulling down method<sup>6,7</sup>, combustion synthesis method<sup>8,9</sup>, thermal explosion spraying<sup>10-12</sup> and so on. In addition, the mechanical properties of the Al<sub>2</sub>O<sub>3</sub>-ZrO<sub>2</sub> eutectic ceramics are mainly decided by microstructure which is influenced significantly by the cooling rate of the melt.

Rapid solidification technique was usually used to prepare metal, alloy and metallic eutectic because it has the high cooling rate greater than 10<sup>5</sup>~10<sup>6</sup>K/s<sup>13-15</sup>. However, this method was rarely to prepare eutectic ceramics due to the high melting points of the ceramics. In this paper, thermal explosion spraying was used to realize rapid solidification for eutectic ceramics, which was a new kind of method for high-efficient heating process. By utilizing the highly exothermic reaction between reactants, the thermal explosion spraying can generate a large amount of heat and gas, and the reaction product can melt easily and be sprayed rapidly under high gas pressure. Once encounter the cool substrates, the high-temperature melt can be solidified quickly. Compared to the traditional rapid quenching method<sup>16</sup>, it has the advantages of simplifying process and saving cost and energy<sup>17,18</sup>. Moreover, this method can reach super high temperatures to realize rapid solidification of the system without any special crucible or extra heating device.

In this paper, Al<sub>2</sub>O<sub>3</sub>-ZrO<sub>2</sub> hypoeutectic coating was prepared by thermal explosion spraying to realize rapid solidification. The heat transfer mechanism of the solidification process was simulated by Finite Element Analysis. The microstructure evolution of the coating under different cooling rates was studied.

### 2. Experimental Procedure

Aluminum (5μm, ≥ 99% in purity) and zirconium nitrate (Zr(NO<sub>3</sub>)<sub>4</sub>, A.R. ≥ 99% in purity) powders were used as raw materials in this experiment. The reactant powders were thoroughly dried and mixed by ball milling for 12~24 hours using alumina milling-media, and then the mixed powders were encased into the explosive spraying reaction equipment. The reaction in this study was expected to take place as follows:



In Addition, certain amount of Al<sub>2</sub>O<sub>3</sub> and ZrO<sub>2</sub> were added to control the reaction temperature of the system. The reactants were ignited by the heat released by the Ni-Cr resistance wire with an 10A electrical current. Once ignited, the reaction instantly generated a large amount of heat, and the system was rapidly heated to a temperature above the melting point of each substance. Meanwhile large quantities of nitrogen produced by the reaction generated a high pressure in the apparatus, so that the melt can spray from the nozzle to the Cu-plate, and the Al<sub>2</sub>O<sub>3</sub>/ZrO<sub>2</sub> hypoeutectic coating was obtained by at rapid cooling rates, as shown in Figure 1.

\*e-mail: zhengyt@hit.edu.cn

The phase composition of the as-sprayed coating was identified by X-ray diffraction (D/MAX-rB, Rigaku, Japan). The cross-sectional microstructure of the coating was investigated by SEM (FE-SEM, S-4700, Hitachi, Japan), EDS (EDAX, USA) and TEM (JEM 2010, Jeol, Japan).

### 3. Results and Discussion

#### 3.1. Phase composition of the coating

The X-ray diffraction pattern of the as-sprayed coating was shown in Figure 2. It showed that the Reaction 1 proceeded as expected and the reactant was transformed to Al<sub>2</sub>O<sub>3</sub> and ZrO<sub>2</sub> completely. The reaction between Al and Zr(NO<sub>3</sub>)<sub>4</sub> generated a large amount of heat and nitrogen. As a result, the reaction temperature could reach about 3000-4000K. Due to the higher oxidizability of oxygen than nitrogen and sufficient oxygen supply, Al was oxidized to form Al<sub>2</sub>O<sub>3</sub> and no aluminum nitride was observed in the product. Because

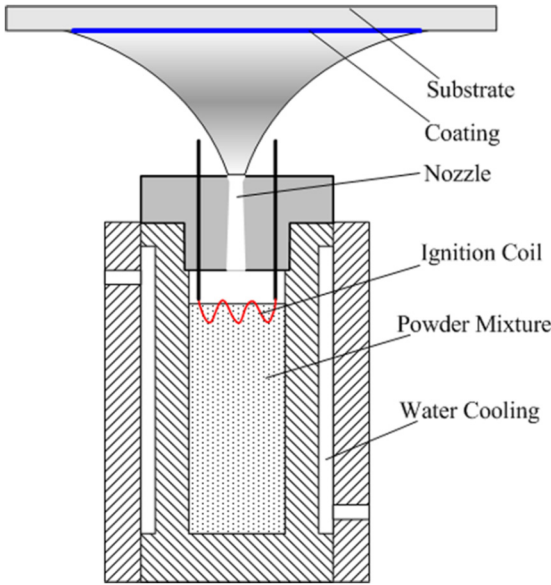


Figure 1. The device of fabricating the Al<sub>2</sub>O<sub>3</sub>/ZrO<sub>2</sub> hypoeutectic coating by thermal explosion spraying.

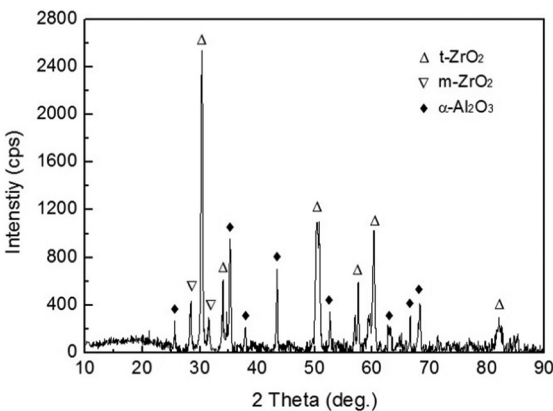


Figure 2. XRD pattern of the Al<sub>2</sub>O<sub>3</sub>-ZrO<sub>2</sub> coating.

of the high cooling rate of the coating, most of the ZrO<sub>2</sub> reserved the tetragonal structure, and the residual showed monoclinic structure. The existence of t-ZrO<sub>2</sub> was beneficial to improve the mechanical properties through transformation toughening of t-ZrO<sub>2</sub> to m-ZrO<sub>2</sub><sup>[19,20]</sup>.

#### 3.2. Microstructure of the coating

The back scattering electron micrograph of the cross-section of the Al<sub>2</sub>O<sub>3</sub>/ZrO<sub>2</sub> hypoeutectic coating was shown in Figure 3. The white particles in the figure were Fe, which was formed by the erosion of the nozzle caused by molten Al<sub>2</sub>O<sub>3</sub>/ZrO<sub>2</sub> during the spraying.

According to the microstructure evolution along the growth direction, Al<sub>2</sub>O<sub>3</sub>/ZrO<sub>2</sub> hypoeutectic coating could be divided into four areas: amorphous structure area, nano-crystalline area, cellular crystal area and dendrite crystal area. The boundaries and the center points of the four areas were marked by numbers 1~9, as shown in Figure 3. The changes of the temperature over time as well as the cooling rate of the marked points were shown in Figure 4a, b, respectively. With the increase of the distance to the surface of Cu-plate, the cooling rate decreased rapidly. Because of the different cooling rates, the crystallization morphologies of Al<sub>2</sub>O<sub>3</sub>/ZrO<sub>2</sub> coating in different areas were varied significantly.

The amorphous structure, which is shown in Figure 3, occurred in the interface contacted with the Cu-plate. In this area, the maximum cooling rate of  $1.68\sim 7.76 \times 10^5 \text{K/s}$  was appeared, as shown in curve 2, 3 in Figure 4a. The temperature of the Cu-plate was much lower than that of the Al<sub>2</sub>O<sub>3</sub>/ZrO<sub>2</sub> melt so that the heat was transferred to Cu-plate rapidly. As a result, the temperature of the melt dropped suddenly to much lower than the glass transition temperature ( $T_g$ ), and then the amorphous structure formed when the atoms were frozen at the place where they were in the liquid.

The cooling rate decreased with the thickness increasing of the Al<sub>2</sub>O<sub>3</sub>/ZrO<sub>2</sub> eutectic coating. When the cooling rate reached about  $0.48\sim 1.68 \times 10^5 \text{K/s}$ , as shown in curve 4, 5 in Figure 4a, there has a certain period of time to allow the atomic diffusion over a short distance, and therefore crystal

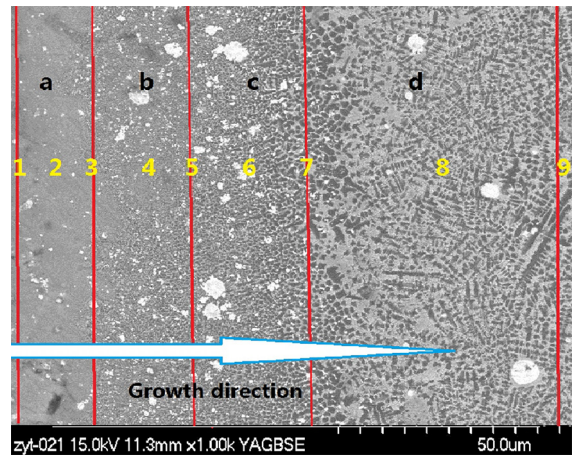
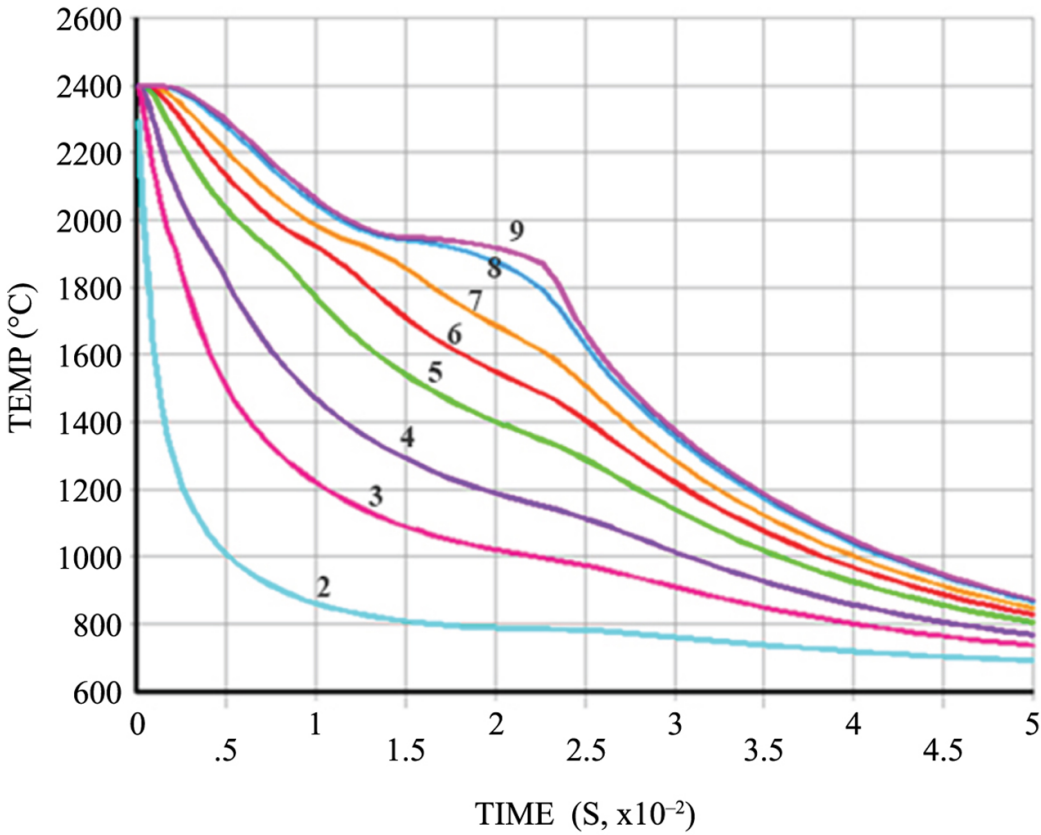


Figure 3. Back scattering electron image of the cross-section of the Al<sub>2</sub>O<sub>3</sub>/ZrO<sub>2</sub> coating (a) amorphous structure (b) nano-crystalline (c) cellular crystal (d) dendrite crystal.



(a)

The cooling rate table

mark points	2	3	4	5	6	7	8	9
cooling rate x 10 <sup>5</sup> k/s	7.76	1.68	0.85	0.48	0.35	0.26	0.16	0.14

(b)

**Figure 4.** The temperature over time (a) and the cooling rate at solidification temperature (b) of mark points during Al<sub>2</sub>O<sub>3</sub>/ZrO<sub>2</sub> melt solidification.

nucleation process was promoted and Al<sub>2</sub>O<sub>3</sub> nano-crystalline formed finally. Nano-scale Al<sub>2</sub>O<sub>3</sub> particles, as shown in Figure 5a, were observed through TEM in crystalline area b in Figure 3. The particle diameters were about 50-100 nm. The microstructure of the nano-crystalline area showed that Al<sub>2</sub>O<sub>3</sub> phases were embedded in the Al<sub>2</sub>O<sub>3</sub>/ZrO<sub>2</sub> hypoeutectic structure matrix. Figure 5b showed the strong boundary combination between the crystal and amorphous area in the coating.

As the thickness increasing of the Al<sub>2</sub>O<sub>3</sub>/ZrO<sub>2</sub> coating, the cooling rate further reduced, and the material diffusion became easier. The nano-sized Al<sub>2</sub>O<sub>3</sub> phase gradually grew up

to form cellular crystal. The cooling rate of cellular crystal area (c area in Figure 3) was about 0.26~0.48 × 10<sup>5</sup>K/s (as shown as curve 6, 7 in Figure 4). X. Mao et al.<sup>21</sup> pointed out that the higher cooling rate decreased the local solidification time and hindered the nucleus grow fully to dendrites, therefore only cellular crystal could be formed, as shown in Figure 6a. The phase formation of Al<sub>2</sub>O<sub>3</sub> precipitated ZrO<sub>2</sub> to solid-liquid interface during the process of nucleation. When the Al<sub>2</sub>O<sub>3</sub> and ZrO<sub>2</sub> proportion in the solid-liquid interface was closed to the eutectic composition, hypoeutectic structure was formed.

Transition region of Nano-crystalline and cellular structure of the Al<sub>2</sub>O<sub>3</sub>/ZrO<sub>2</sub> coating was shown in Figure 6b. Cellular

$\text{Al}_2\text{O}_3$  with diameter of about  $1\sim 2\mu\text{m}$  were embedded in  $\text{Al}_2\text{O}_3/\text{ZrO}_2$  hypoeutectic matrix.

When the last part of the melt was sprayed, the cooling rate slowed down to the minimum value of  $0.14\sim 0.26 \times 10^5\text{K/s}$  (as shown in curve 8, 9 in Figure 4). The latent heat of the crystallization helped the fully grown  $\text{Al}_2\text{O}_3$  cellular crystal to form the secondary dendrite arm and the dendrites. The dendrite region of crystal structure showed that  $\text{Al}_2\text{O}_3$  dendrites were embedded in the  $\text{Al}_2\text{O}_3/\text{ZrO}_2$  hypoeutectic structure matrix.

Dendrite  $\text{Al}_2\text{O}_3$  crystal structure was shown in Figures 7 and 8, respectively. Figure 7 showed the early stage of the dendrite formation. In this stage pseudo-eutectics formed and dendrite became less due to the high cooling rate.  $\text{Al}_2\text{O}_3$  dendrite was

embedded in the light gray  $\text{Al}_2\text{O}_3/\text{ZrO}_2$  eutectic matrix, which was demonstrated by EDS shown in Figure 7. When platform of the cooling curve appeared, the low cooling rate and the usual law of solidification conducted the dendrite to form the final morphology. Hypoeutectic products of  $\text{Al}_2\text{O}_3$  and  $\text{ZrO}_2$  were greatly deviated from the eutectic composition, so that a large area of alumina dendrites was formed as shown in Figure 8.

Owing to the characteristics of thermal spraying technique, pores can readily form and deteriorated the properties of the coating. However, the  $\text{Al}_2\text{O}_3/\text{ZrO}_2$  hypoeutectic coating prepared by thermal explosion spraying showed a high relative density and no pores were observed. High relative density of the coating prepared in this experiment was

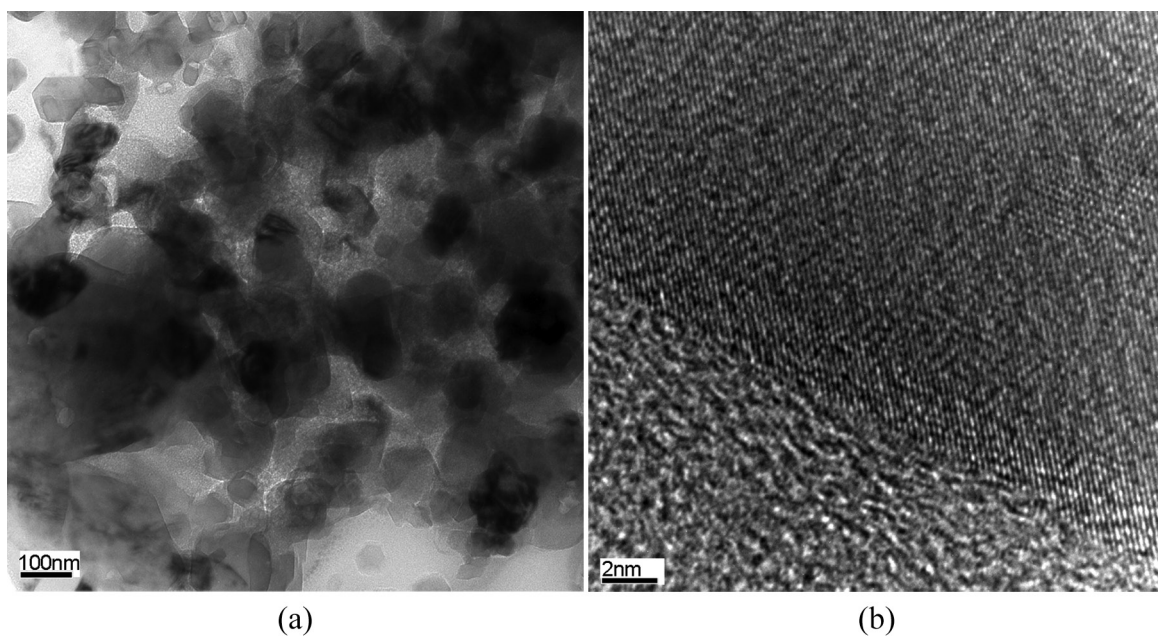


**Figure 5.** TEM images of (a) nanostructured  $\text{Al}_2\text{O}_3$  crystal and (b) boundary of amorphous and crystal particle.

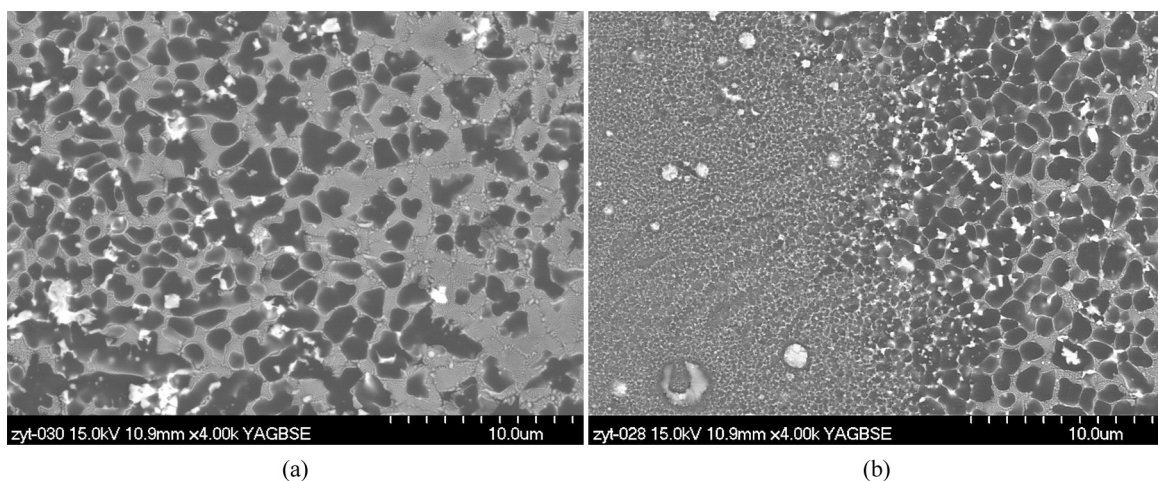


**Figure 6.** Back scattering electron images of (a) cellular structure and (b) nano and cellular structure of the  $\text{Al}_2\text{O}_3/\text{ZrO}_2$  coating.

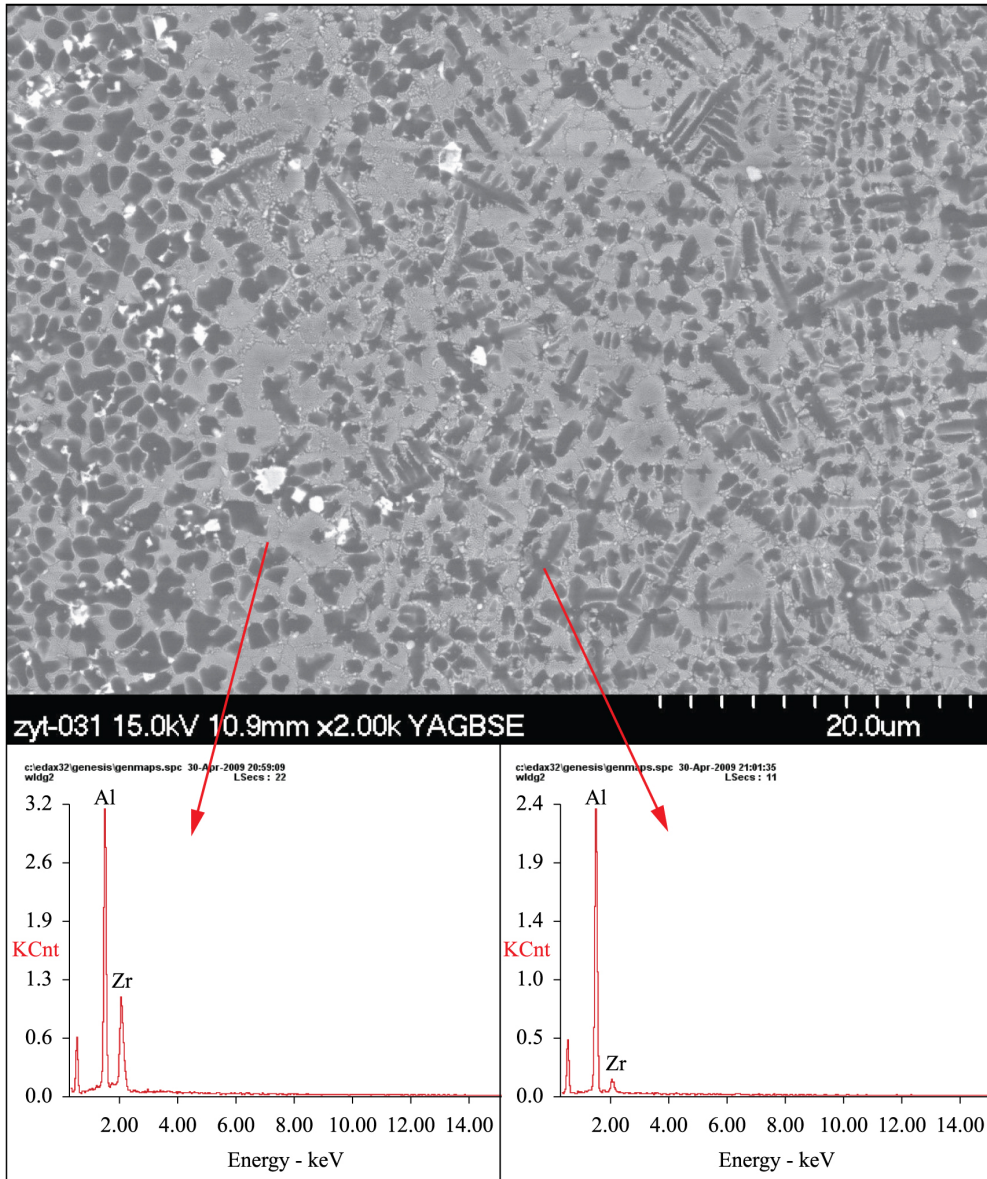


Figure 7. Back scattering electron image and EDS of the dendrite crystal.

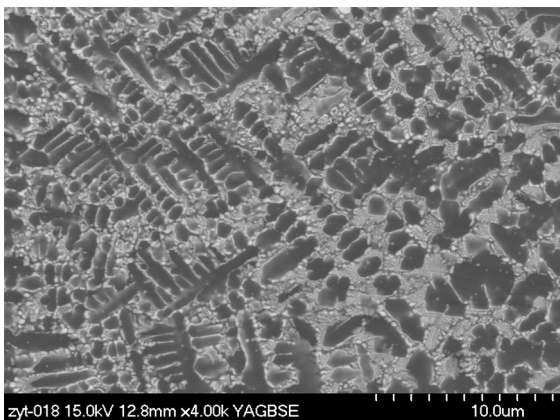


Figure 8. Back scattering electron image of the dendrite crystal.

attributed to the strong impact on the coating bring from the explosion spraying, which is favorable for the densification of the coating.

#### 4. Conclusions

Rapid solidification of  $Al_2O_3/ZrO_2$  melt at super high temperature was realized by explosion spraying method. With the increase of distance to the surface of Cu-plate, the cooling rate of the melt solidification decrease gradually and the microstructure evolution of coating could be divided into four crystalline areas: amorphous structure, nano-crystalline, cellular crystal and dendrite crystal. Different cooling rates of these crystalline regions were simulated by Finite Element Analysis.

## Reference

1. Waku Y, Nakagawa N, Wakamoto T, Ohtsubo H, Shimizu K and Kohtoku Y. A ductile ceramic eutectic composite with high strength at 1873. *Nature*. 1997; 389(6646):49-52. <http://dx.doi.org/10.1038/37937>.
2. LLorca JL, Pastor JY, Poza P, Pena JI, Francisco I, Larrea A, et al. Influence of the Y<sub>2</sub>O<sub>3</sub> content and temperature on the mechanical properties of melt-grown Al<sub>2</sub>O<sub>3</sub>-ZrO<sub>2</sub> eutectics. *Journal of the American Ceramic Society*. 2004; 87(4):633-639. <http://dx.doi.org/10.1111/j.1551-2916.2004.00633.x>.
3. Lee JH, Yoshikawa A, Kaiden H, Lebbou K, Fukuda T, Yoon DH, et al. Microstructure of Y<sub>2</sub>O<sub>3</sub> doped Al<sub>2</sub>O<sub>3</sub>/ZrO<sub>2</sub> eutectic fibers grown by the micro-pulling-down method. *Journal of Crystal Growth*. 2001; 231(1-2):179-185. [http://dx.doi.org/10.1016/S0022-0248\(01\)01451-8](http://dx.doi.org/10.1016/S0022-0248(01)01451-8).
4. Mesa MC, Oliete PB, Pastor JY, Martín A and LLorca J. Mechanical properties up to 1900 K of Al<sub>2</sub>O<sub>3</sub>/Er<sub>3</sub>Al<sub>5</sub>O<sub>12</sub>/ZrO<sub>2</sub> eutectic ceramics grown by the laser floating zone method. *Journal of the European Ceramic Society*. 2014; 34(9):2081-2087. <http://dx.doi.org/10.1016/j.jeurceramsoc.2013.11.013>.
5. Larrea A, de la Fuente GF, Merino RI and Orera VM. ZrO<sub>2</sub>-Al<sub>2</sub>O<sub>3</sub> eutectic plates produced by laser zone melting. *Journal of the European Ceramic Society*. 2002; 22(2):191-198. [http://dx.doi.org/10.1016/S0955-2219\(01\)00279-5](http://dx.doi.org/10.1016/S0955-2219(01)00279-5).
6. Su HJ, Zhang J, Cui CJ, Liu L and Fu HZ. Rapid solidification of Al<sub>2</sub>O<sub>3</sub>-Y<sub>3</sub>Al<sub>5</sub>O<sub>12</sub>-ZrO<sub>2</sub> eutectic in situ composites by laser zone remelting. *Journal of Crystal Growth*. 2007; 30(2):448-456. <http://dx.doi.org/10.1016/j.jcrysgro.2007.06.029>.
7. Lee JH, Yoshikawa A, Kaiden H, Lebbou K, Fukuda T, Yoon DH, et al. Microstructure of Y<sub>2</sub>O<sub>3</sub> doped Al<sub>2</sub>O<sub>3</sub>/ZrO<sub>2</sub> eutectic fibers grown by the micro-pulling-down method. *Journal of Crystal Growth*. 2001; 231(1-2):179-185. [http://dx.doi.org/10.1016/S0022-0248\(01\)01451-8](http://dx.doi.org/10.1016/S0022-0248(01)01451-8).
8. LLorca J, Pastor JY, Poza P, Peña JI, Francisco I and Larrea A. Influence of the Y<sub>2</sub>O<sub>3</sub> content and temperature on the mechanical properties of melt-grown Al<sub>2</sub>O<sub>3</sub>-ZrO<sub>2</sub> eutectics. *Journal of the American Ceramic Society*. 2004; 87(4):633-639. <http://dx.doi.org/10.1111/j.1551-2916.2004.00633.x>.
9. Zhao ZM, Zhang L, Zheng J, Bai H, Zhang S and Xu B. Microstructure and mechanical properties of Al<sub>2</sub>O<sub>3</sub>/ZrO<sub>2</sub> composite produced by combustion synthesis. *Scripta Materialia*. 2005; 53(8):995-1000. <http://dx.doi.org/10.1016/j.scriptamat.2005.06.016>.
10. Zhao ZM, Zhang L, Song YG and Wang W. Al<sub>2</sub>O<sub>3</sub>/ZrO<sub>2</sub>(Y<sub>2</sub>O<sub>3</sub>) self-growing composite prepared by combustion synthesis under high gravity. *Scripta Materialia*. 2008; 58(3):207-211. <http://dx.doi.org/10.1016/j.scriptamat.2007.09.051>.
11. Zheng YT, Li HB and Zhou T. Microstructure and mechanism of Al<sub>2</sub>O<sub>3</sub>/ZrO<sub>2</sub> eutectic coating prepared by combustion-assisted thermal explosion spraying. *Applied Surface Science*. 2011; 258(4):1531-1534. <http://dx.doi.org/10.1016/j.apsusc.2011.09.125>.
12. Zheng YT, Li HB, Zhou T, Zhao J and Yang P. Microstructure and mechanical properties of Al<sub>2</sub>O<sub>3</sub>/ZrO<sub>2</sub> eutectic ceramic composites prepared by explosion synthesis. *Journal of Alloys and Compounds*. 2013; 551:475-480. <http://dx.doi.org/10.1016/j.jallcom.2012.11.064>.
13. Li Y, Liu HY, Davies HA and Jones H. Easy glass formation in Mg<sub>64</sub>Ni<sub>21</sub>Nd<sub>15</sub> by bridgman solidification. *Materials Science and Engineering A*. 1994; 179-180:628-631. [http://dx.doi.org/10.1016/0921-5093\(94\)90281-X](http://dx.doi.org/10.1016/0921-5093(94)90281-X).
14. Jones H. Enhancement of properties and performance of materials by rapid solidification processing. *Key Engineering Materials*. 1995; 97-98:1-12. <http://dx.doi.org/10.4028/www.scientific.net/KEM.97-98.1>.
15. Guan SK and Wang LG. Research and development trend of rapidly solidified alloy. *Modern Casting*. 2004; 4:22-26.
16. Han YH, Yun J, Harada Y, Makino T and Kakegawa K. Eutectic structure from amorphous Al<sub>2</sub>O<sub>3</sub>-ZrO<sub>2</sub>-Y<sub>2</sub>O<sub>3</sub> system by rapid quenching technique for potential hybrid solar cell application. *Advances in Applied Ceramics*. 2010; 109(2):101-103. <http://dx.doi.org/10.1179/174367509X12554402490949>.
17. Wei MX, Wang SQ, Wang F and Cui XH. A thermal explosion process to fabricate an intermetallic matrix composite coating on a steel. *Materials & Design*. 2009; 30(8):3041-3047. <http://dx.doi.org/10.1016/j.matdes.2008.12.013>.
18. Klinger L, Gotman I and Horvitz D. In situ processing of TiB<sub>2</sub>/TiC ceramic composites by thermal explosion under pressure: experimental study and modeling. *Materials Science and Engineering A*. 2001; 302(1):92-99. [http://dx.doi.org/10.1016/S0921-5093\(00\)01359-9](http://dx.doi.org/10.1016/S0921-5093(00)01359-9).
19. Tuan WH, Chen RZ, Wang TC, Cheng CH and Kuo PS. Mechanical properties of Al<sub>2</sub>O<sub>3</sub>/ZrO<sub>2</sub> composites. *Journal of the European Ceramic Society*. 2002; 22(16):2827-2833. [http://dx.doi.org/10.1016/S0955-2219\(02\)00043-2](http://dx.doi.org/10.1016/S0955-2219(02)00043-2).
20. Hannink RHJ, Kelly PM and Muddle BC. Transformation toughening in zirconia-containing ceramics. *Journal of the American Ceramic Society*. 2000; 83(3):461-487. <http://dx.doi.org/10.1111/j.1151-2916.2000.tb01221.x>.
21. Mao XM, Li JG and Fu HZ. Effect of local solidification time on the dendrite-to-cell transition at high growth rates. *Materials Science and Engineering A*. 1994; 183(1-2):233-238. [http://dx.doi.org/10.1016/0921-5093\(94\)90907-5](http://dx.doi.org/10.1016/0921-5093(94)90907-5).